Check for updates

Geophysical Research Letters

RESEARCH LETTER
10.1029/2023GL102834

On a Possible Mechanism of Space Stem Formation in Negative Long Sparks

Xiangen Zhao[1], Nikolay A. Popov[2], Quan Gan[3], Yuxuan Ding[1], Yaping Du[1], and Junjia He[4]

[1]Department of Building Environment and Energy Engineering, The Hong Kong Polytechnic University, Hong Kong, China, [2]Skobel'tsyn Institute of Nuclear Physics, Moscow State University, Moscow, Russia, [3]Three Gorges Power Plant, China Three Gorges Corporation, Yichang, China, [4]State Key Laboratory of Advanced Electromagnetic Engineering and Technology, Huazhong University of Science and Technology, Wuhan, China

Key Points:

- Only a section of the local luminous region at the primary corona streamer boundary is heated to form a space stem, but not all of it
- The temperature field of a space stem is reconstructed for the first time and presents a non-uniform distribution
- A secondary ionization wave may contribute to the space stem formation at the primary corona streamer burst boundary

Supporting Information:

Supporting Information may be found in the online version of this article.

Correspondence to:

X. Zhao and Y. Du,
zhaoxiangen@outlook.com;
ya-ping.du@polyu.edu.hk

Citation:

Zhao, X., Popov, N. A., Gan, Q., Ding, Y., Du, Y., & He, J. (2023). On a possible mechanism of space stem formation in negative long sparks. *Geophysical Research Letters*, *50*, e2023GL102834. https://doi.org/10.1029/2023GL102834

Received 11 JAN 2023
Accepted 3 APR 2023

Author Contributions:

Data curation: Quan Gan
Formal analysis: Xiangen Zhao, Nikolay A. Popov, Yuxuan Ding
Funding acquisition: Yaping Du, Junjia He
Investigation: Nikolay A. Popov, Quan Gan, Junjia He
Methodology: Xiangen Zhao, Quan Gan
Supervision: Nikolay A. Popov, Yaping Du, Junjia He
Visualization: Xiangen Zhao
Writing – original draft: Xiangen Zhao, Nikolay A. Popov, Yuxuan Ding, Yaping Du

© 2023. The Authors.
This is an open access article under the terms of the Creative Commons Attribution-NonCommercial-NoDerivs License, which permits use and distribution in any medium, provided the original work is properly cited, the use is non-commercial and no modifications or adaptations are made.

Abstract To study the mechanism of space stem formation, the high-speed direct imaging technique and Schlieren photography are used to simultaneously observe the space stems in a 1.35-m air gap under the lightning impulse voltage. It is found that the average length and diameter of the space stem is approximately 5 and 0.5 mm, which is about 1/3 of the length and 1/10 of the diameter of the local luminous region respectively. Moreover, the space stem exhibits a non-uniform distributed temperature with a maximum value of several hundred Kelvin for tens of microseconds. Accordingly, a possible mechanism is proposed that the space stem is formed at the primary corona streamer boundary as a result of the propagation of a secondary ionization wave from the HV electrode and survives long enough (to finish the polarization) due to the fast gas heating and production of atomic oxygen.

Plain Language Summary It is well known that negative leaders in the air develop in a step-wise manner, with each step originating from a space stem. However, the mechanism of space stem formation is still unknown, one of the main reasons being the lack of experimental observations. For this reason, this paper carries out laboratory research to observe the optical and thermal properties of space stems. The observations reveal that the local luminous region at the primary corona streamer boundary is not fully heated into the space stem, but only about 1/3 of its length. If based on conventional direct images, the measured length and diameter of space stems would be 2.5 and 10 times larger than the actual values, respectively. The reconstructed temperature field shows that the axial temperature and diameter of the space stem are not uniformly distributed, with higher temperatures and smaller diameters at the end away from the HV electrode. Finally, a new possible mechanism is proposed for the space stem formation, in which the secondary ionization wave from the HV electrode contributes to the initial formation of the space stem, and then the voltage changes help the space stem survive long enough to finish the polarization.

1. Introduction

It is well known that negative leaders in air advance in a stepped fashion (Bazelyan & Raizer, 1998; Rakov & Uman, 2003), which is one of the outstanding mysteries in atmospheric electricity. Each step is originated from a bright nucleus in a filamentary corona ahead of the leader tip. This bright nucleus is termed space stem (Bazelyan & Raizer, 1998; Les Renardières Group, 1981), which is the key to leader stepping. The mechanism of space stem formation was summarized in 2014 as one of the top 10 questions in lightning research (Dwyer & Uman, 2014) and remains inconclusive to this day (Kutsyk & Babich, 2021).

Numerous observations have been made for the step characteristics of negative leaders, both in natural lightning (Biagi et al., 2010; Hill et al., 2011; Huang et al., 2018; Petersen & Beasley, 2013; Qi et al., 2016; Wang et al., 2016) and in the laboratory (Kochkin et al., 2014; Kostinskiy et al., 2018; Les Renardières Group, 1981; Ortega et al., 1994; Reess et al., 1995; Xie et al., 2013; Yue et al., 2015). Some of these observations (Kostinskiy et al., 2018) refer to the space stem, but the expression "space stem/leader" is always used in the text, which means that it is not certain that this is the space stem state. However, specific observations of space stems are relatively rare. Reess et al. (1995) observed the origin and development of a space stem with an image converter working in streak mode, and speculated that the space stem should be located at branched points of negative streamers and an adequate positive ion concentration was necessary to produce positive streamers. In addition, Reess et al. (1995) observed the space stem after the primary corona with a Schlieren system, and found that heated channels were

19448007, 2023, 12, Downloaded from https://agupubs.onlinelibrary.wiley.com/doi/10.1029/2023GL102834 by HONG KONG POLYTECHNIC UNIVERSITY HU NG HOM, Wiley Online Library on [10/01/2024]. See the Terms and Conditions (https://onlinelibrary.wiley.com/terms-and-conditions) on Wiley Online Library for rules of use; OA articles are governed by the applicable Creative Commons License

highly discontinuous, and there were cold tracks (hardly visible in Schlieren images) that connected these hot channels to each other and possibly to the cathode. Kochkin et al. (2016) observed the pilot system containing the space stem with an intensified CCD camera, and hypothesized that the positive corona from the beads contributed to the space stem formation. Recently, Zhao, Lee, & He (2021), Zhao et al. (2022) studied the space stem using high-speed Schlieren photography and found that space stems exist in both positive and negative sparks in the air. However, Zhao did not further investigate the mechanism of space stem birth.

Several numerical models (Cooray & Arevalo, 2017; Gallimberti et al., 2002; Guo et al., 2019; Rakotonandrasana et al., 2008; Syssoev et al., 2020) have been proposed to simulate the stepping process of negative leaders. However, these models do not consider the mechanism and process of space stem formation, but mostly use assumptions, for example, Cooray and Arevalo (2017) assumed that a small conducting channel lay at the streamer boundary of the stepped leader as a space stem. It was only in recent years that scholars began to propose possible mechanisms for space stem formation. Wang et al. (2016) proposed that the space stem formation was related to the new corona streamer burst at the boundary of the primary one. This was due to the extension of the primary leader and the electric field enhancement at the boundary of the primary corona streamer burst. Moreover, the polarization should be finished first to produce the system of positive and negative corona streamers to heat the space stem channel. Malagon-Romero and Luque (2019) argued that a new corona streamer burst at the boundary of the primary one was not included in the space stem formation, while the attachment instability inside the primary streamer filament contributed to the space stem formation. Syssoev and Iudin (Iudin et al., 2018; A. Syssoev & Iudin, 2021) believed that the space stem was due to the joint action of electron drifting and ionization processes at the boundary of the primary corona streamer burst, where the strong inhomogeneous stochastic electric field was present.

It seems that available experimental research does not allow reliably unveiling a mechanism for space leader formation (Babich et al., 2021). The aim of this letter is to provide some more refined experimental observations. To this end, the simultaneous direct imaging technique and Schlieren photography are employed in the experiments, and the temperature field of space stems is reconstructed from Schlieren images. A possible mechanism for space stem formation is finally discussed.

2. Methods

All experiments in this paper were carried out on the platform we have previously reported by Zhao, Becerra, et al. (2021), Zhao, Liu, et al. (2021). The experimental layout is detailed in Figure S1 in Supporting Information S1. Only two points will be highlighted here, that is, the choice of voltage waveform and the parameters and synchronization of direct and Schlieren photography.

Reess et al. (1995) proposed that the optimum with respect to observing the space stem formation and development was the 0.3/2,000 μs impulse shape, while the duration of this process was about a few hundred nanoseconds. This time duration far exceeds the temporal resolution of the observation means in this paper. To this end, the lightning impulse voltage is chosen in this paper, under which condition only the space stems are produced and not allowed to continue to develop, facilitating observations. The lightning impulse was generated by a Marx generator, which was with a rise/fall time of 4.3/45.4 μs as shown in Figure S2 in Supporting Information S1.

A high-speed camera Cam1 (Photron FASTCAM SA5-X2) was used for the Schlieren photography, and another high-speed camera Cam2 (Phantom SA5) was for the direct photography. To fully synchronize the exposure sequences of Cam1 and Cam2, a function generator (Sapphire 9,200+) was employed to trigger these two cameras and then both cameras were operated with a speed of 192,308 frames-per-second (fps) and an exposure time of 3.6 μs and a dead time of 1.6 μs. Accordingly, the spatial resolution and the observation area were 180 μm/pixel and 27×46 mm2 for the Schlieren system, while 1.4 mm/pixel and 175×360 mm2 for the direct imaging system.

In the experiments, the testing conditions included a temperature of 300 K, absolute humidity of 22.0 g/m^3 and atmospheric pressure.

3. Results

3.1. Typical Experimental Results

Figure 1 shows typical experimental results under the negative impulse peaked at 200 kV. The exposure sequences in Figure 1a indicate that the two cameras work almost simultaneously. This means that the corresponding direct

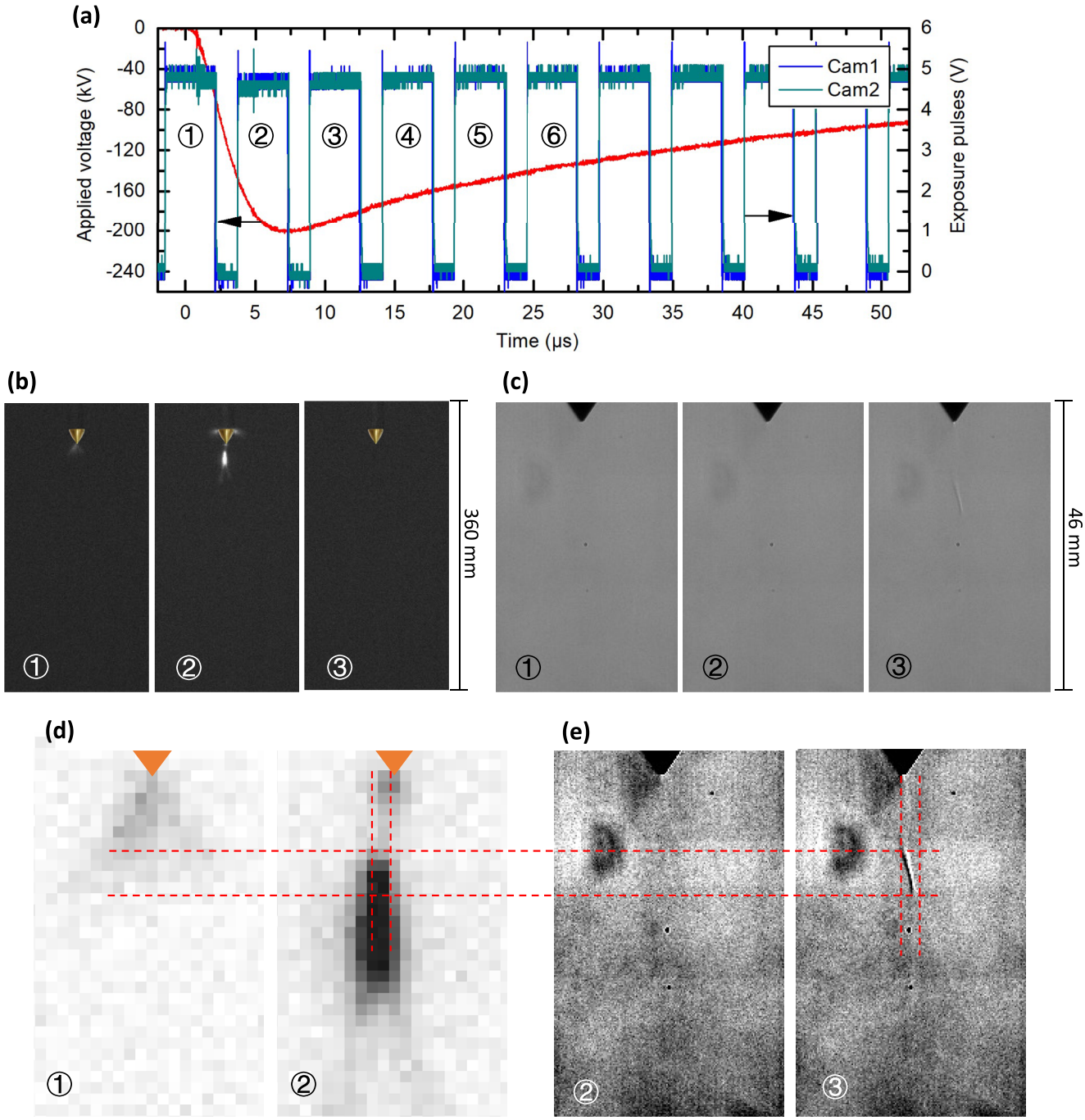

Figure 1. Typical experimental results: (a) The applied voltage, and the exposure sequences of the two high-speed cameras; (b) Original direct images by Cam2; (c) Original Schlieren images by Cam1; Partially enlarged direct images (d) and Schlieren images (e), in which the direct images are color inverted and the Schlieren images are contrast-enhanced. The number of each image corresponds to the timing sequence marked with the same number in (a).

and Schlieren images present the luminosity and density changes of the discharge channel in the same time period. According to the direct images in Figure 1b, the negative streamer burst is produced at the electrode tip before $t = 2.2$ μs (see direct image ①). The second streamer burst is expected to occur between $t = 3.8$ and 7.4 μs (see direct image ②). The reason is that the first streamer burst in image ① typically lasts only a few hundred nanoseconds (Reess et al., 1995), which is less than the dead time between image ① and image ②. After the second streamer burst, an isolated luminous region can be identified, and a ring of corona discharge is also present around the electrode body, which is not concerned here. After $t = 9.0$ μs (such as direct image ③), the discharge

19448007, 2023, 12, Downloaded from https://agupubs.onlinelibrary.wiley.com/doi/10.1029/2023GL102834 by HONG KONG POLYTECHNIC UNIVERSITY HU NG HOM, Wiley Online Library on [10/01/2024]. See the Terms and Conditions (https://onlinelibrary.wiley.com/terms-and-conditions) on Wiley Online Library for rules of use; OA articles are governed by the applicable Creative Commons License

19448007, 2023, 12, Downloaded from https://agupubs.onlinelibrary.wiley.com/doi/10.1029/2023GL102834 by HONG KONG POLYTECHNIC UNIVERSITY HU NG HOM, Wiley Online Library on [10/01/2024]. See the Terms and Conditions (https://onlinelibrary.wiley.com/terms-and-conditions) on Wiley Online Library for rules of use; OA articles are governed by the applicable Creative Commons License

stops, and no significant luminosity is recorded. Correspondingly, the Schlieren images in Figure 1c show that before $t = 2.2$ μs (see Schlieren image ①), no obvious region with density variation is visible at the electrode tip. Between $t = 3.8$ and 7.4 μs (see Schlieren image ②), however, a small region of density change starts to appear at the electrode tip with a length of approximately 0.54 mm. After $t = 9.0$ μs (see Schlieren image ③), an isolated heated region appears ahead of the electrode tip. According to the traditional definition that the luminous nucleus formed in the zone previously covered by the corona streamers but isolated from the leader tip in long negative sparks is called "space stem" (Les Renardières Group, 1981), the isolated luminous region in Figure 1b ② and the isolated heated region in Figure 1c ③ can be called a space stem.

To further confirm the relative position and size of the isolated luminous region and the isolated heated region, Figures 1d and 1e shows locally enlarged images of both, keeping all images the same size. We can find several interesting phenomena. First, the isolated luminous region presumably starts at the primary corona streamer boundary. Second, the isolated heated region is not along all isolated luminous regions, but only a part of the latter closer to the HV electrode. Third, appearance of channel density variations lags behind channel luminosity by about 1.6 μs (or the dead time of the camera). Note that the light-emitting and heating are synchronous and last for about several hundred nanoseconds (Popov, 2011), while the drop in gas density begins only when the gas-dynamic rarefaction of the hot channel occurs. For the case in Figure 1e with a radius of $R = 300$–400 μm at a temperature $T_g = 400$–500 K, the characteristic gas-dynamic time $\tau_g = R/C_s \approx 1$ μs, where C_s is the speed of sound in air (Popov, 2011).

Note that the observations by Kochkin et al. (2016) suggest that the space stems appear as luminous beads, which are different from the thin filaments in Figure 1e. This may be attributable to differences in the spatial resolution of the observing system. The spatial resolution of the Schlieren system used in this paper is 180 μm/pixel, and the average value of the space stem is about 5 mm. However, the spatial resolution of the observing systems used in the literature (e.g., Les Renardières Group, 1981; Reess et al., 1995) is on the order of cm, or even m, which means that the spatial stem occupies only one pixel point in the images captured by these systems, and therefore looks more like a bead.

Similar phenomena are present in other groups of experiments. In the Supporting Information S1, another two sets of experiments are shown in Figures S3 and S4 in Supporting Information S1 with 2 and 3 space stems, respectively.

3.2. Temperature Field of the Space Stem

According to the modern concepts (Bazelyan & Raizer, 1998), the space stem is a plasma formation capable of initiating positive and negative streamer flashes. One of the important point of the mechanism of streamer initiation is the polarization of the space stem plasma, which leads to an increase in the electric field at its poles and the formation of positive and negative streamers. The polarization time τ_P of a plasma channel with length L and radius r can be estimated with $\tau_P \approx \tau_M \cdot (L/2r)^2/\ln(L/r)$, where $\tau_M = 1/4\pi\sigma$—Maxwellian time (Bazelyan & Raĭzer, 2000). At the conditions such as $P = 1$ atm and $L/r = 20$ (see Figure 1), the space stem polarization occurs rather quickly ($\tau_p < 1$ μs) if the electron density N_e in the channel is larger than 3×10^{10} cm^{-3}. However, in the air at room temperature and pre-breakdown fields, it is impossible to maintain such an electron density at microsecond times due to the rapid attachment of electrons to oxygen molecules. While it is possible to significantly increase the lifetime of air plasma in the discharge channel by the gas heating and by generating of O-atoms (Liu, 2012), which is involved in the destruction of negative ions. That is why the data on the dynamics of gas heating, which can be obtained by the Schlieren technique, are of particular importance.

The discharge channel temperature is estimated with the method detailed in He et al. (2022), Liu et al. (2021), Zhao, Becerra, et al. (2021), first to determine whether the isolated section in Figure 1 is a space stem, and second to investigate its thermal characteristics. Figure 2a plots the temperature field of the isolated heated channel in Figure 1c, which is not over 700 K. That is, the isolated segment observed in Figure 1 is a space stem. Furthermore, results in Figure 2a show that the temperature field of the space stem is not uniform, with its highest temperature distributed at the end away from the HV electrode. In addition, the closer to the HV electrode, the space stem gradually increases in cross-section. From these measurements, in particular, it follows that this heated region cannot be called a "space leader," since the distinguishing feature of the leader channel is that the dominant process of the charged particle production is thermal (rather than the electric field) ionization (Bazelyan & Raizer, 1998). At a temperature of less than 1000 K, this is impossible.

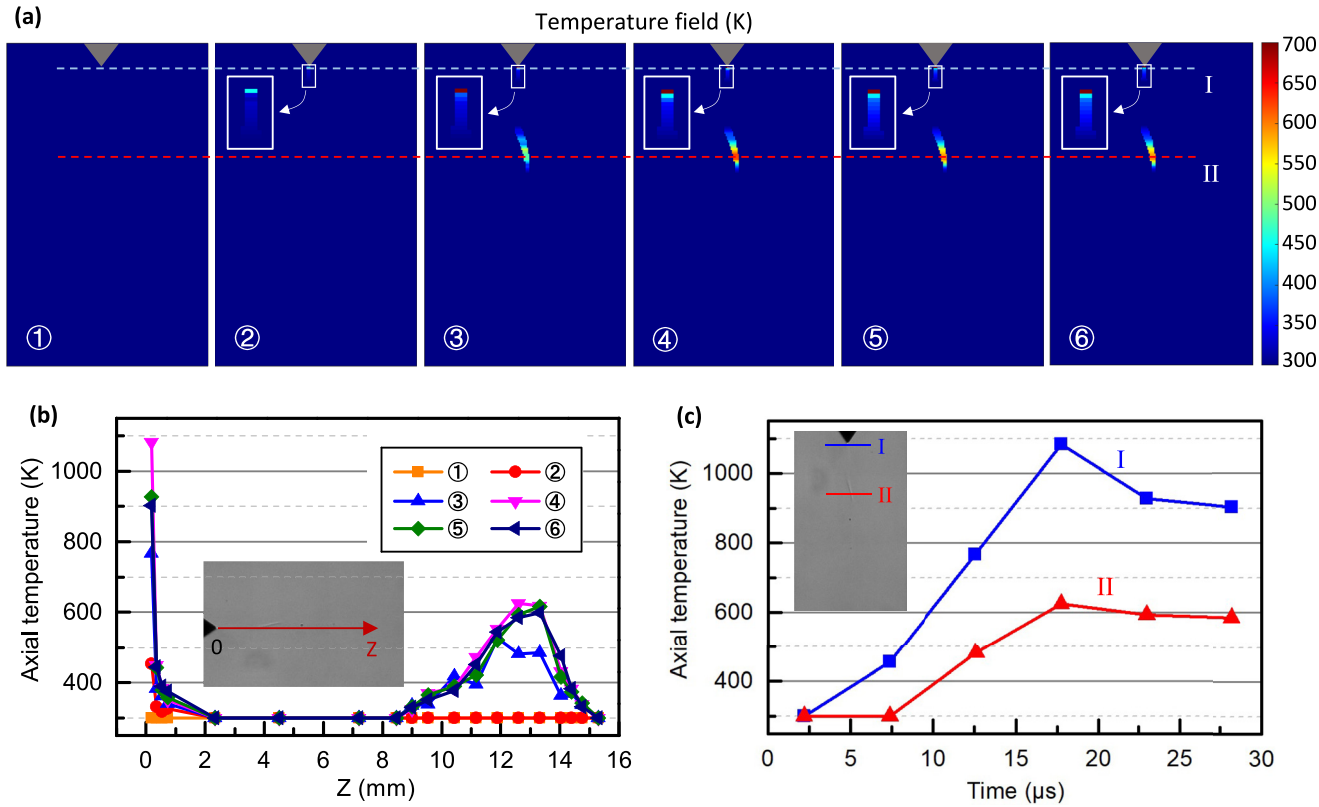

Figure 2. Temperature reconstruction from Schlieren images for the case in Figure 1. (a) Temperature field evolution over time, and the number of each image corresponds to the timing sequence marked with the same number in Figure 1a. (b) Time-varying axial maximum temperature distribution of the discharge channel. (c) Time-varying maximum temperatures for typical cross-sections of the main channel and the space stem.

To demonstrate the discharge channel temperature more quantitatively, the time-varying maximum temperature distribution along the air gap direction is calculated and shown in Figure 2b, where the electrode tip is defined as the coordinate origin. It can be seen that the gas heating is mainly around the electrode tip and at the space stem, while the temperature between them remains essentially room temperature. Moreover, the maximum gas temperature at the electrode tip is higher than that of the space stem. More specifically, Figure 2c shows the axial temperature evolution of two typical cross-sections. The results show that the electrode tip region starts to be heated at $t = 2.2$ μs and reaches a maximum value of about 1084 K at $t = 17.8$ μs, while the space stem region starts to be heated at $t = 7.4$ μs and also reaches a maximum value of about 622 K at $t = 17.8$ μs. Note that the color scale in Figure 2a only goes up to 700 K, which is to allow the temperature distribution of the space stems to be better identified. Subsequently, the discharge stops, and the axial temperature gradually decreases at both cross-sections, which should be attributed to the heat conduction effect being greater than the vibrational-translational relaxation effect (Cheng et al., 2020).

The data in Figure 2 make it possible to evaluate the parameters of hot regions. For the space stem, to heat the gas by $\Delta T = 300$ K in electric fields $E/N = 100$ Td, the required value of the specific input energy is approximately equal to $W = 0.6$ eV/molecule (under the assumption that the fraction of discharge energy spent on fast gas heating is about 15% (Popov, 2011)). In this case, the density of atomic oxygen, which estimates the efficiency of VT-relaxation of $N_2(v)$, will be $[O] \approx 10^{18}$ cm^{-3} (considering that the energy cost of O-atoms production in air at $E/N = 100$ Td is approximately 10 eV per atom (Popov & Starikovskaia, 2022)).

3.3. Morphology of Space Stems

Observations in Figure 1 show that the space stem exhibits some dimensional differences in the direct image and the Schlieren image, which are specifically investigated in this section. Figure 3a shows the optical and thermal lengths of space stems. Statistically, in the experiments of this paper, the optical length ranges from 7.0 to

19448007, 2023, 12, Downloaded from https://agupubs.onlinelibrary.wiley.com/doi/10.1029/2023GL102834 by HONG KONG POLYTECHNIC UNIVERSITY HU NG HOM, Wiley Online Library on [10/01/2024]. See the Terms and Conditions (https://onlinelibrary.wiley.com/terms-and-conditions) on Wiley Online Library for rules of use; OA articles are governed by the applicable Creative Commons License

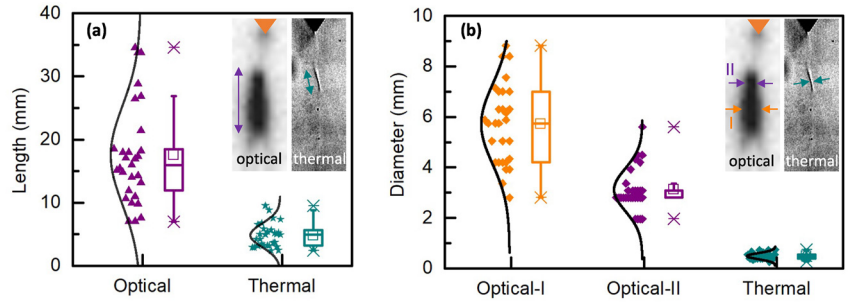

Figure 3. Optical and thermal dimensions of the space stem: (a) Length and (b) Diameter.

34.6 mm with an average of 17.5 mm, while the thermal length is from 2.4 to 9.5 mm with an average of 4.8 mm. Figure 3b illustrates the optical and thermal diameters of space stems. In this case, two optical diameters are defined, one corresponding to the maximum optical diameter in the heated region (see optical-I in Figure 3b) and the other corresponding to the maximum optical diameter in the unheated region (see optical-II in Figure 3b). The statistical results show that the optical diameter I ranges between 2.8 and 8.8 mm with a mean value of 5.7 mm, while the optical diameter II ranges from 2.0 to 5.6 mm with a mean value of 3.1 mm. However, the thermal diameter is between 0.3 and 0.7 mm with a mean value of 0.5 mm. Note that the thermal diameter is almost 10 times smaller than the optical diameter, which may be due to the contraction of discharge channel as a result of the development of ionization-heating instability.

Strictly by its definition (Malagon-Romero & Luque, 2019), a space stem should refer to the isolated region that is heated, rather than the isolated region that is illuminated. Therefore, thermal dimensions are more appropriate for describing the space stem morphology. As can be seen from Figure 3, if the space stem morphology is estimated from the optical image, the length will be 2.5 times more biased, and the diameter will be 10 times more biased.

4. Discussions

The mechanism of space stem formation is among the most current topics of interest (Babich et al., 2021). Although it fails to capture the space stem formation process due to the limited temporal resolution in this paper, a possible mechanism for the space stem formation is proposed by combining test results and plasma theory, which is diagrammed in Figure 4.

In the phase I, after the end of the primary corona streamer burst or primary ionization wave, a secondary ionization wave may be triggered by a disturbance near the HV electrode, such as a sudden change of electric field due

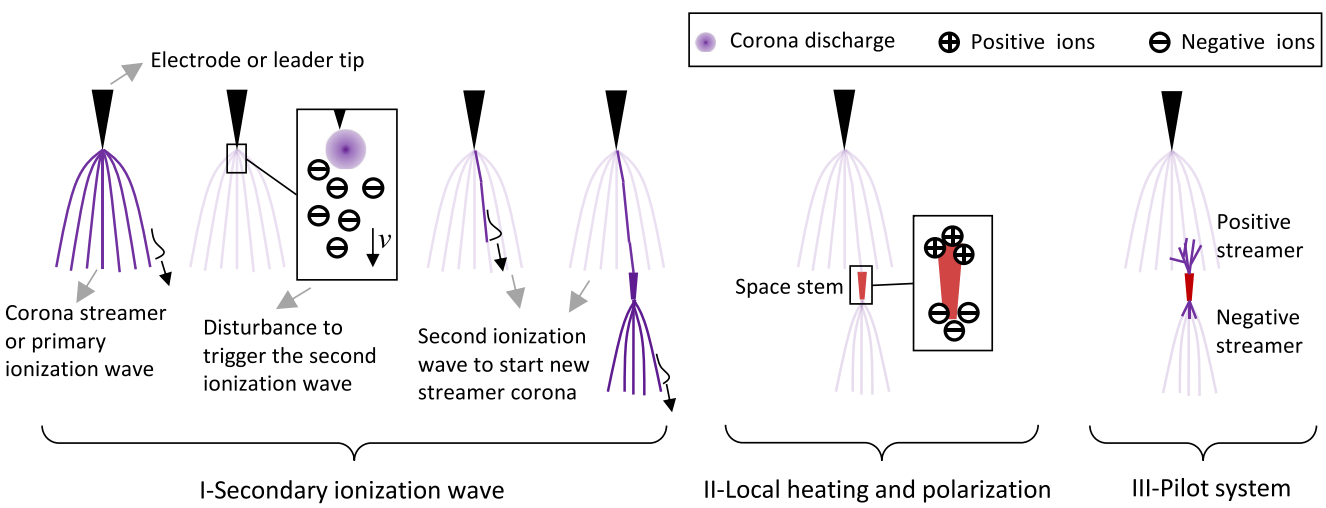

Figure 4. Schematic diagram of the proposed mechanism of space stem formation in negative long sparks.

19448007, 2023, 12, Downloaded from https://agupubs.onlinelibrary.wiley.com/doi/10.1029/2023GL102834 by HONG KONG POLYTECHNIC UNIVERSITY HU NG HOM, Wiley Online Library on [10/01/2024]. See the Terms and Conditions (https://onlinelibrary.wiley.com/terms-and-conditions) on Wiley Online Library for rules of use; OA articles are governed by the applicable Creative Commons License

19448007, 2023, 12, Downloaded from https://agupubs.onlinelibrary.wiley.com/doi/10.1029/2023GL102834 by HONG KONG POLYTECHNIC UNIVERSITY HU NG HOM, Wiley Online Library on [10/01/2024]. See the Terms and Conditions (https://onlinelibrary.wiley.com/terms-and-conditions) on Wiley Online Library for rules of use; OA articles are governed by the applicable Creative Commons License

to a corona discharge there. The formation mechanism of such an ionization wave in spark discharges at applied voltages $dU/dt > 40–50$ kV/μs was studied by Bazelyan and Popov (Aleksandrov & Bazelyan, 2000; Bazelyan & Popov, 2020). This secondary ionization wave propagates along the previously created streamer filament and significantly increases its conductivity. This can explain why there is a thin glowing channel between the localized luminous region and the HV electrode in our observations (see images ② in Figure 1a, Figures S3b–S5b in Supporting Information S1). Furthermore, the secondary ionization wave can lead to a significant electric field increase at the head of the glowing channel, and triggers a new corona streamer burst there. That may be the reason why the localized luminous region appears at the boundary of the primary corona streamer burst (see images ① and ② in Figure 1b).

In the phase II, the increasing voltage across the discharge gap ensures the injection of charges into the discharge gap. The movement of these charges produces the current that flows through the plasma channel, providing a sufficiently high level of conductivity of this channel and, accordingly, gas heating and dissociation of oxygen molecules (Bazelyan & Popov, 2020). As a result, a long-lived (compared to the polarization times) plasma region (or space stem), is formed. The fact that the gas heating occurs only in a certain limited area of the formed space stem in Figure 2 may be due to that the radius of the space stem channel becomes larger as it approaches the HV electrode. Accordingly, the current density decreases, which leads to a decrease in specific energy input and gas heating (Popov, 2001). This may be the reason for the following two findings, that is, no space stems could be observed when the voltage rise time was greater than 15 μs (Reess et al., 1995), and space stems occur more frequently under lightning impulse voltages than under switching impulse voltages (Zhao, Lee, & He, 2021; Zhao et al., 2022).

In the phase III, after the polarization, the electric field at the space stem's poles is enhanced, resulting in the conditions for the start of a system of positive and negative streamers. The current flowing through the space stem is provided by the movement of charged streamer heads (Bazelyan & Raizer, 1998). This current can be the main cause of gas heating in the space stem region, which leads to the development of ionization-heating instability and then the formation of a space leader. The phase III were not observed in our experiments, which is an inference from the existing knowledge (e.g., Gallimberti et al., 2002; Ortega et al., 1994).

Although the space stem polarize quickly (less than 1 μs in our experiments according to the calculations by Bazelyan and Raĭzer (2000)), new space stems can be generated in front of this space stem before it is transformed into a space leader, that is, cascaded space stems, provided that the applied voltage rises fast enough. As the applied voltage amplitude increases to 360 kV, the cascaded space stems can be found frequently in Schlieren images, with typical results detailed in Figure S5 in Supporting Information S1. Liu et al. (2022) suggest that the generation of lightning initial breakdown pulses may be due to the cascaded space stems and connections between them.

Note that the above discussion is based on the laboratory observations of this paper, namely the space stems generated around the electrode. It is believed that this space stem formation process may also occur in natural lightning, although electrodes are not present in lightning. The leader, due to its high conductivity, can be regarded as an extension of the electrode (Kekez & Savic, 1976) and, by the same token, the leader head can be equated to some extent with the electrode tip. After the negative leader has completed one step, an intense corona streamer appears at the main leader head (Qi et al., 2016; Wang et al., 2016), creating a condition similar to the phase I in Figure 4. The subsequent processes can therefore also occur during the next step of the lightning discharge. Existing natural lightning observations cannot support this inference, and observations with higher temporal and spatial resolution are needed in the future work.

In this work, the formation of localized hot channels (~600 K) in the streamer zone of a negative spark discharge is experimentally shown, therefore, the main emphasis was placed on the analysis of the parameters of these channels and their possible influence on the development of the discharge.

5. Conclusions

In this letter, laboratory experiments were carried out to observe the space stem in long negative sparks. Using simultaneously the direct imaging technique and Schlieren photography, the luminosity and the air density variations were visualized, and the temperature field was reconstructed. A possible mechanism for space stem formation is finally proposed. Some main conclusions are as follows.

1. The length and diameter of space stem estimated from the direct images are approximately 2.5 and more than 10 times bigger than those from the Schlieren images, respectively. To observe the space stem morphology, Schlieren photography is recommended.
2. The thermal properties of the space stem are not uniformly distributed, that is, the thermal diameter decreases, and the temperature increases as further away from the HV electrode. In addition, the space stem can be at a temperature of hundreds of Kelvin for tens of microseconds.
3. The space stem starts at the primary corona streamer boundary, and cascaded space stems can be present.
4. The propagation of a secondary ionization wave from the HV electrode contributes to the space stem formation, and the gas heating and the atomic oxygen production play an important role in a significant increase in its lifetime and in the polarization of the space stem.

Data Availability Statement

The data can be accessed at the WDC for Geophysics, Beijing (https://doi.org/10.12197/2023GA002).

Acknowledgments
The work leading to this paper was supported by the Postdoc Matching Fund Scheme of PolyU and the National Natural Science Foundation of China (51821005). The work of NP is supported by the Russian Science Foundation (23-17-00264).

References

Aleksandrov, N., & Bazelyan, E. (2000). Step propagation of a streamer in an electronegative gas. *Journal of Experimental and Theoretical Physics*, *91*(4), 724–735. https://doi.org/10.1134/1.1326965

Babich, L., Kutsyk, I., Bochkov, E., Koehn, C., & Neubert, T. (2021). *General processes responsible for the space leader birth in streamer coronas of negative leaders*. Plasma Research Express.

Bazelyan, E. M., & Popov, N. A. (2020). Stepwise development of a positive long spark in the air. *Plasma Physics Reports*, *46*(3), 293–305. https://doi.org/10.1134/s1063780x20030022

Bazelyan, E. M., & Raizer, Y. P. (1998). *Spark discharge*. CRC Press.

Bazelyan, E. M., & Raĭzer, Y. P. (2000). The mechanism of lightning attraction and the problem of lightning initiation by lasers. *Physics-Uspekhi*, *43*(7), 701–716. https://doi.org/10.1070/pu2000v043n07abeh000768

Biagi, C. J., Uman, M. A., Hill, J. D., Jordan, D. M., Rakov, V. A., & Dwyer, J. (2010). Observations of stepping mechanisms in a rocket-and-wire triggered lightning flash. *Journal of Geophysical Research*, *115*(D23), D23215. https://doi.org/10.1029/2010jd014616

Cheng, C., Liu, L., He, H., Luo, B., Hu, J., Chen, W., & He, J. (2020). Experimental study of the dynamics of leader initiation with a long dark period. *Journal of Physics D: Applied Physics*, *53*(20), 205203. https://doi.org/10.1088/1361-6463/ab7625

Cooray, V., & Arevalo, L. (2017). Modeling the stepping process of negative lightning stepped leaders. *Atmosphere*, *8*(12), 245. https://doi.org/10.3390/atmos8120245

Dwyer, J. R., & Uman, M. A. (2014). The physics of lightning. *Physics Reports*, *534*(4), 147–241. https://doi.org/10.1016/j.physrep.2013.09.004

Gallimberti, I., Bacchiega, G., Boudiou-Clergerie, A., & Lalande, P. (2002). Fundamental processes in long air gap discharges. *Comptes Rendus Physique*, *3*(10), 1335–1359. https://doi.org/10.1016/s1631-0705(02)01414-7

Guo, Z., Li, Q., Bretas, A., & Rakov, V. A. (2019). A simplified physical model of negative leader in long sparks. *Electric Power Systems Research*, *176*, 105955. https://doi.org/10.1016/j.epsr.2019.105955

He, J., Wang, X., Zhao, X., Lee, J., Du, Y., Liu, X., et al. (2022). Schlieren techniques for observations of long positive sparks: Review and application. *High Voltage*, *7*(5), 1–15. https://doi.org/10.1049/hve2.12225

Hill, J. D., Uman, M. A., & Jordan, D. M. (2011). High-speed video observations of a lightning stepped leader. *Journal of Geophysical Research*, *116*(D16), D16117. https://doi.org/10.1029/2011jd015818

Huang, H., Wang, D., Wu, T., & Takagi, N. (2018). Formation features of steps and branches of an upward negative leader. *Journal of Geophysical Research: Atmospheres*, *123*(22), 12597–12605. https://doi.org/10.1029/2018jd028979

Iudin, D., Syssoev, A., & Popov, N. (2018). Generation of stems in streamer corona of negative leader. *Paper presented at the proceedings of XVI international conference on atmospheric electricity*.

Kekez, M. M., & Savic, P. (1976). Laboratory simulation of the stepped leader in lightning. *Canadian Journal of Physics*, *54*(22), 2216–2224. https://doi.org/10.1139/p76-266

Kochkin, P., Lehtinen, N., P J van Deursen, A., & Østgaard, N. (2016). Pilot system development in metre-scale laboratory discharge. *Journal of Physics D: Applied Physics*, *49*(42), 425203. https://doi.org/10.1088/0022-3727/49/42/425203

Kochkin, P. O., van Deursen, A. P. J., & Ebert, U. (2014). Experimental study of the spatio-temporal development of metre-scale negative discharge in air. *Journal of Physics D: Applied Physics*, *47*(14), 145203. https://doi.org/10.1088/0022-3727/47/14/145203

Kostinskiy, A. Y., Syssoev, V. S., Bogatov, N. A., Mareev, E. A., Andreev, M. G., Bulatov, M. U., et al. (2018). Abrupt elongation (stepping) of negative and positive leaders culminating in an intense corona streamer burst: Observations in long sparks and implications for lightning. *Journal of Geophysical Research: Atmospheres*, *123*(10), 5360–5375. https://doi.org/10.1029/2017jd027997

Kutsyk, I., & Babich, L. (2021). Heating of a local region of a branching streamer as a starting point of a space leader and a negative-leader step. *Plasma Physics Reports*, *47*(3), 251–256. https://doi.org/10.1134/s1063780x21030089

Les Renardières Group. (1981). *Negative discharges in long air gaps at Les Renardieres, 1978 results*. Electra.

Liu, N. (2012). Multiple ion species fluid modeling of sprite halos and the role of electron detachment of O in their dynamics. *Journal of Geophysical Research*, *117*(A3), A03308. https://doi.org/10.1029/2011ja017062

Liu, N., Scholten, O., Hare, B. M., Dwyer, J. R., Sterpka, C. F., Kolmašov, I., & Santolík, O. (2022). LOFAR observations of lightning initial breakdown pulses. *Geophysical Research Letters*, *49*(6), e2022GL098073. https://doi.org/10.1029/2022gl098073

Liu, X., Wang, X., Zhao, X., Xiao, P., Liu, Y., & He, J. (2021). An improved inversion algorithm to reconstruct 2D temperature fields of long sparks with high-speed schlieren technique. *Measurement*, *180*, 109620. https://doi.org/10.1016/j.measurement.2021.109620

Malagon-Romero, A., & Luque, A. (2019). Spontaneous emergence of space stems ahead of negative leaders in lightning and long sparks. *Geophysical Research Letters*, *46*(7), 4029–4038. https://doi.org/10.1029/2019gl082063

Ortega, P., Domens, P., Gibert, A., Hutzler, B., & Riquel, G. (1994). Performance of a 16.7 m air rod-plane gap under a negative switching impulse. *Journal of Physics D: Applied Physics*, *27*(11), 2379–2387. https://doi.org/10.1088/0022-3727/27/11/019

19448007, 2023, 12, Downloaded from https://agupubs.onlinelibrary.wiley.com/doi/10.1029/2023GL102834 by HONG KONG POLYTECHNIC UNIVERSITY HU NG HOM, Wiley Online Library on [10/01/2024]. See the Terms and Conditions (https://onlinelibrary.wiley.com/terms-and-conditions) on Wiley Online Library for rules of use; OA articles are governed by the applicable Creative Commons License

Petersen, D. A., & Beasley, W. H. (2013). High-speed video observations of a natural negative stepped leader and subsequent dart-stepped leader. *Journal of Geophysical Research: Atmospheres*, *118*(21), 12110–112119. https://doi.org/10.1002/2013jd019910

Popov, N. (2001). Investigation of the mechanism for rapid heating of nitrogen and air in gas discharges. *Plasma Physics Reports*, *27*(10), 886–896. https://doi.org/10.1134/1.1409722

Popov, N. (2011). Fast gas heating in a nitrogen–oxygen discharge plasma: I. Kinetic mechanism. *Journal of Physics D: Applied Physics*, *44*(28), 285201. https://doi.org/10.1088/0022-3727/44/28/285201

Popov, N., & Starikovskaia, S. (2022). Relaxation of electronic excitation in nitrogen/oxygen and fuel/air mixtures: Fast gas heating in plasma-assisted ignition and flame stabilization. *Progress in Energy and Combustion Science*, *91*, 100928. https://doi.org/10.1016/j.pecs.2021.100928

Qi, Q., Lu, W., Ma, Y., Chen, L., Zhang, Y., & Rakov, V. A. (2016). High-speed video observations of the fine structure of a natural negative stepped leader at close distance. *Atmospheric Research*, *178–179*, 260–267. https://doi.org/10.1016/j.atmosres.2016.03.027

Rakotonandrasana, J. H., Beroual, A., & Fofana, I. (2008). Modelling of the negative discharge in long air gaps under impulse voltages. *Journal of Physics D: Applied Physics*, *41*(10), 105210. https://doi.org/10.1088/0022-3727/41/10/105210

Rakov, V. A., & Uman, M. A. (2003). *Lightning: Physics and effects*. Cambridge University Press.

Reess, T., Ortega, P., Gibert, A., Domens, P., & Pignolet, P. (1995). An experimental study of negative discharge in a 1.3 m point-plane air gap: The function of the space stem in the propagation mechanism. *Journal of Physics D: Applied Physics*, *28*(11), 2306–2313. https://doi.org/10.1088/0022-3727/28/11/011

Syssoev, A., & Iudin, D. (2021). On a possible mechanism of space stem formation at the negative corona streamer burst periphery. *Atmospheric Research*, *259*, 105685. https://doi.org/10.1016/j.atmosres.2021.105685

Syssoev, A. A., Iudin, D. I., Bulatov, A. A., & Rakov, V. A. (2020). Numerical simulation of stepping and branching processes in negative lightning leaders. *Journal of Geophysical Research: Atmospheres*, *125*(7), e2019JD031360. https://doi.org/10.1029/2019jd031360

Wang, D., Takagi, N., Uman, M., & Jordan, D. (2016). Luminosity progression in dart-stepped leader step formation. *Journal of Geophysical Research: Atmospheres*, *121*(24), 14612–614620. https://doi.org/10.1002/2016jd025813

Xie, Y., He, H., & He, J. (2013). Observation of leader development in rod–rod air gaps under negative switching impulse. *Japanese Journal of Applied Physics*, *52*(9R), 090206. https://doi.org/10.7567/jjap.52.090206

Yue, Y., He, H., Chen, W., He, J., Wu, C., Zhao, X., & Huo, F. (2015). Characteristics of long air gap discharge current subjected to switching impulse. *CSEE Journal of Power and Energy Systems*, *1*(3), 49–58. https://doi.org/10.17775/cseejpes.2015.00035

Zhao, X., Becerra, M., Yang, Y., & He, J. (2021). Elongation and branching of stem channels produced by positive streamers in long air gaps. *Scientific Reports*, *11*(1), 1–11. https://doi.org/10.1038/s41598-021-83816-7

Zhao, X., Gan, Q., Du, Y., Lee, J., Li, Z., Wang, X., et al. (2022). Observation of isolated heating segments ahead of the discharge channel under positive and negative lightning impulses. In *Paper presented at the 2022 36th international conference on lightning protection (ICLP)*.

Zhao, X., Lee, J., & He, J. (2021). High-speed schlieren photographic observations of space stems in negative and positive sparks. In *Paper presented at the 2021 35th international conference on lightning protection (ICLP) and XVI international symposium on lightning protection (SIPDA)*.

Zhao, X., Liu, X., Yang, Y., Wang, X., Liu, Y., & He, J. (2021). Observations of the channel illuminations during dark periods in long positive sparks. *Geophysical Research Letters*, *48*(4), e2020GL091815. https://doi.org/10.1029/2020gl091815

References From the Supporting Information

IEC 60060-1. (2010). High-voltage test techniques Part 1: General definitions and test requirements (3rd ed.).

Zhao, X., He, J., He, H., Yue, Y., & Chen, W. (2016). Number and dimensional distribution of stems near the anode in a 1m air gap under positive pulse. In *Paper presented at the 33th international conference on lightning protection*.

Zhao, X., Liu, L., Yue, Y., He, H., Liu, L., & He, J. (2019). On the use of quantitative Schlieren techniques in temperature measurement of leader discharge channels. *Plasma Sources Science and Technology*, *28*(7), 075012. https://doi.org/10.1088/1361-6595/ab1c3e

19448007, 2023, 12, Downloaded from https://agupubs.onlinelibrary.wiley.com/doi/10.1029/2023GL102834 by HONG KONG POLYTECHNIC UNIVERSITY HU NG HOM, Wiley Online Library on [10/01/2024]. See the Terms and Conditions (https://onlinelibrary.wiley.com/terms-and-conditions) on Wiley Online Library for rules of use; OA articles are governed by the applicable Creative Commons License